Homogenised constitutive model coupling damage and debonding for reinforced concrete structures under cyclic solicitations

François Voldoire, Christelle Combescure, Hélène Dumontet

CrossMark

Homogenised constitutive model coupling damage and debonding for reinforced concrete structures under cyclic solicitations

Christelle Combescure [a,b,c], Hélène Dumontet [c], François Voldoire [a,b,*]

[a] Électricité de France, R&D/AMA, 1, Avenue du Général de Gaulle, F-92141 Clamart, France
[b] Laboratoire de Mécanique des Structures Industrielles Durables, UMR EDF – CNRS – CEA 8193, 1, Avenue du Général de Gaulle, F-92141 Clamart, France
[c] Univ. Paris VI, UMR CNRS 7190, Institut Jean Le Rond d'Alembert, 4, place Jussieu, F-75252 Paris Cedex 05, France

A B S T R A C T

A new stress resultant constitutive model for reinforced concrete plates under cyclic solicitations is presented. This model is built by the periodic homogenisation approach using the averaging method and couples damage of concrete and periodic debonding between concrete and steel rebar. In one-dimensional situations, we derive a closed-form solution of the local problem useful to verify and set up the plate problem. The one dimensional macroscopic constitutive model involves a limited number of parameters, the sensibility of which is studied. Comparison to experimental results underlines the pertinence of the model by considering internal debonding in order to properly represent the mechanical dissipation occurring during cyclic loadings on reinforced concrete panels.

© 2013 Elsevier Ltd. All rights reserved.

1. Introduction

Reinforced concrete (RC) is an intensively used material in civil engineering. The structural strength analysis of RC buildings, both at the conceptual design stage and for re-examination during the life duration, demands more and more sophisticated means, but adapted to engineering practice needs, especially when justifying safety margins and eventually determining design weaknesses, for existing structures and buildings. Thus Nonlinear Finite Element Analyses are used to determine the load carrying capacity of RC structures and buildings, for both monotonic and cyclic loading paths, as needed by complex in-service or accidental loading scenarios, as earthquakes. A lot of researches have been carried out to propose appropriate constitutive models, fitted to the kinematical description of RC structural elements and their Finite Element formulation. Most of these researches address RC members and columns, for which efficient and robust modeling for engineering purposes are available; nevertheless it seems that rather less research works are devoted to RC panel (slabs and walls) modeling, aiming at performing complex full scale building seismic analyses.

First, we propose in the following a quick literature survey in order to outline the state of the art concerning both main RC structural element behavioural features and RC modeling and generic constitutive modeling approaches, as a prerequisite to set out the aims of our work.

1.1. Overall context and experimental observations

RC is a composite material, in which the needed strength in tension, which cannot be reached by the plain concrete alone, susceptible to cracking, is provided by steel rebar. Due to concrete matrix and steel rebar behaviours and to the bond action between both materials, complex redistributions of mechanical fields occur between these two material phases; thanks to this effect, the cracked RC is stiffer than steel rebar alone. However, this feature leads to stiffness degradation and energy dissipation, of great consequence for the seismic analysis. The contribution of steel rebar and their bond with cracked concrete, in the overall behaviour of the RC section, is called "tension-stiffening", see for instance Feenstra and De Borst (1995) and Marti et al. (1998). For many decades, each component of the composite material that is RC, were studied closely and several conclusions can be sorted out:

– the concrete matrix undergoes stiffness degradation and strain softening by cracking in tension. A non-symmetrical response stems from opening and closing of cracks, and lateral confine-

* Corresponding author at: Électricité de France, R&D/AMA, 1, Avenue du Général de Gaulle, F-92141 Clamart, France. Tel.: +33 147654321.
E-mail addresses: christelle.combescure@edf.fr (C. Combescure), helene.dumontet@upmc.fr (H. Dumontet), francois.voldoire@edf.fr (F. Voldoire).

ment effect (Sheikh and Uzumeri, 1982) from steel stirrups, ties and hoops affects concrete strength. Residual strains and crushing appear in compression (Farrar and Baker, 1992), followed by crack shear transfer (due to aggregate interlocking), dilatancy, and dowel action effect for more complex loading paths;

– the bond action between concrete matrix and steel rebar, which can be analysed through bar pull-out tests, produces local cracking, due to geometrical singularities. The elastic moduli mismatch between both phases induces debonding beyond a certain loading level. Those behaviours cause, under cyclic solicitations, a quick degradation of stiffness and strength, and energy dissipation as shown in CEB-FIP code (1993) or by Fardis (2009). Therefore, the bond action plays a major role in the hysteretic behaviour of RC structures as recognised for a long time (Mörsch, 1909);

– the steel rebar itself involves elastoplasticity, and buckling, see CEB-FIP code (1993) or Spacone et al. (1996). In usually designed RC structural elements, these nonlinearities arise in the vicinity of the overall collapse of the whole RC section.

Regarding the context imposed by the considered applications, we need to draw the following phenomena-ranking table. First, the analyses conducted are restrained to RC structural element cyclic loading associated to engineering needs for low and moderate seismicity regions. As a consequence, the collapse phenomena are excluded. Therefore, it will be considered hereafter that neither yielding nor buckling of steel rebar, nor even crushing of concrete occurs. It is assumed that the defect evolution – i.e. micro-cracks– in concrete during monotonic or cyclic stress state transients addresses the elastic stiffness degradation as shown by Farrar and Baker (1992), while the progressive debonding between concrete and steel rebar produces residual strains (CEB-FIP code, 1993 ; Kobayashi et al., 1980). Of course, non symmetrical behaviour observed in tensile–compressive loading directions in the concrete phase has to be accounted for, stemming from the alternate opening and closing of concrete cracks. Concrete confinement effect will be only considered as an input parameter for strength values. As far as that goes, we do not consider geometrical non-linearities (like P-Delta effect (Rutenberg, 1982)), nor viscous or rate effects on concrete behaviour (velocities remaining low in seismic range), nor specific inertial effects at the microscopic scale (frequencies remaining low in seismic range). Inertial forces are determined from a simple weighted averaging mass density and overall accelerations in the RC section.

According to experimental observations, quoted in Carpinteri and Carpinteri (1984) and Favre et al. (1990) and Maekawa et al. (2003), the bond stress-slip constitutive relation is the same whatever the direction of loading is, the rebar pulling-out criterion being reached prior to the steel yielding one for usual designs. Moreover, a simple yet rational bond-slip model for the bond behaviour between reinforcement bars and concrete proposed by Ingraffea et al. (1984) is adopted as a reference. According to this work, and following other authors from this time, it is assumed that non-linear bond-slip mechanism occurring is correlated to an internal micro-cracks system, located in the vicinity of steel rebar in plain concrete between two successive transverse steel bars where macro cracks can grow due to the singularity induced by the elastic coefficient mismatch (Goto, 1971). As a consequence, the bond slipping is induced by prior concrete cracking. As in classical rebar pull-out test, we presume that this bond-slip mechanism can be idealised by a two-scale approach. For ordinary ribbed rebar, a simple stepped rigid-perfectly plastic bond stress-slip relationship could be satisfactory as done by Marti et al. (1998) and Pimentel et al. (2010).

1.2. Overall context of constitutive modeling

According to the different scales of analysis, many constitutive models are proposed in scientific literature and disseminated to practitioners for industrial applications on RC buildings or structural elements. In each case considered, the range of applications and the one of loading levels (small nonlinearities or failure modes determination...) are crucial criteria to avoid excessive or unsuitable computational burden or inappropriate results output. Such models can be arranged in the following classes as proposed by Spacone et al. (1996):

– for local refined analysis devoted to member joints or other local geometric singularities, a two phases modeling is preferred, involving sophisticated constitutive relations for concrete (damage models and smeared cracking, softening-induced uniqueness lost regularisation treatment...), for steel rebar (plasticity...), and for steel–concrete bond (adhesion). Nevertheless, this kind of FEM simulations needs refined meshes and suffers from iterative procedures convergence issues, due to the softening behaviour; therefore, in our view, such approach cannot be reasonably proposed for whole building analyses;

– at the intermediate scale, it can be suggested, for instance, multilayer modeling for RC panels, slabs and walls, or multi-fibre modeling for RC members, where simplified constitutive relations of both materials are implemented (Ngo and Scoderlis, 1967; Guedes et al., 1994; Spacone et al., 1996) and in which the nonlinear behaviour of bond might be merged with the steel reinforcement plastic behaviour;

– for overall building or main RC frame analyses, "homogenised" or "globalised" RC models for members, beams and columns, and lumped hinge nonlinear models are often proposed. These models summarise the main aspects of the nonlinear response (e.g. Takeda et al., 1970) at the scale of the whole building, and their parameters are calibrated with reference to experimental results and a limited number of characteristic material data.

Therefore, we can identify two main ways to formulate these constitutive models for RC structure behaviour:

– for local refined analysis and intermediate scale models, the usual way consists in developing a series of theoretical expressions idealising each elementary phenomenon involved in the overall behaviour and calibrated from a series of experimental data. The RC constitutive model is then built by addition of each elementary mechanism. RC panels, for instance, have to be modelled as multi-component structural systems: concrete, reinforcing bars and interaction between these two phases. This is the way used by many authors, namely Lee (2011), Marti et al. (1998), Okamura and Kim (2000), Pimentel et al. (2010), Selby and Vecchio (1997), Soltani et al. (2005), Spacone and El-Tawil (2004) and Vecchio and Collins (1986). The main hypothesis of this first family of local refined analysis constitutive models consists in the superposition of stress distribution stemming from each phase and the interface stress; see for instance Feenstra and De Borst (1995);

– for "globalised" RC models, the preferred approach consists in developing the constitutive model from an a priori general framework in order to formulate, in a consistent way, the state equations and the evolution laws and to define the intrinsic mechanical dissipation. Moreover, a homogenisation technique or multi-scale analysis, see for instance Andrieux et al. (1986), Caillerie (1995), Perić et al. (2011) and Suquet (1993), can be used in order to transfer the physical variables and equations

from the microscopic scale to the macroscopic one, i.e. from the multi-phase description to the resultant state of the RC structure section.

Among all of these developments, some are conducted according to the theoretical framework of Simple Materials presented by Germain (1973a,b), Thermodynamics of irreversible processes, see Coleman and Gurtin (1967) and Germain et al. (1983) and Generalised Standard Materials theory (GSM) see for instance Chaboche (2003), Dragon and Mròz (1979), Halphen and Nguyen (1975) and Lemaître and Chaboche (1990).

The latter is the usual framework of the associated rate-independent plasticity or damage mechanics. It is the way used by many authors, for instance Alliche and Dumontet (2011), Badel et al. (2007), Lorentz and Godard (2011), Dragon and Mròz (1979), Gatuingt and Pijaudier-Cabot (2002), Rumanus and Meschke (2007, 2008), Shao et al. (2006), to formulate their constitutive models and especially to idealise the plain concrete behaviour. The adequacy with experimental observations is used to calibrate the model parameters, accepting a certain compromise level. The GSM framework for nonlinear constitutive equations incorporates a well-define energetic characterisation and is well adapted to be implemented through an time integration algorithm associated with a well-posed minimisation problem, by an implicit way in any Finite Element software. This adequacy with the numerical implementation persists even with the softening behaviour of concrete, which introduces an additional difficulty, by uniqueness loss and localisation at the equilibrium equations stage, consequently spatial mesh dependency. This peculiar feature requires specific methods, among them nonlocal formulations: Pijaudier-Cabot and Bažant (1987), Lorentz and Andrieux (2003) and Lorentz and Godard (2011).

Most of constitutive models dealing with RC structures seismic behaviour proposed in literature are devoted to members, beams and columns, including the collapse prediction, see for instance Banon et al. (1981), Carpinteri and Carpinteri (1984), Guedes et al. (1994), Maekawa et al. (2003), Ngo and Scoderlis (1967), Spacone et al. (1996), Spacone and El-Tawil (2004) Takeda et al. (1970). Indeed, these structural elements are the most representative of actual RC building throughout the world, and are studied in particular to assess the population protection against the seismic risk. Due to this particular geometry, the most popular way is to formulate constitutive models in the "intermediate scale" context by means of multi-fibre beam models.

However, several authors addressed their works to formulate RC panel constitutive equations, most of them using a "local refined analysis" point of view: Brun et al. (2003), Kotronis et al. (2003), Krätzig and Polling (2004), Mazars et al. (2002), Selby and Vecchio (1997), Soltani et al. (2003). Indeed, especially in industrial and large RC building, RC panels are often used in order to increase both stiffness and dissipative properties of the building, two properties desired for their aseismic design. Nevertheless, at the authors' knowledge, there is very few available constitutive models formulated in that general framework, including GSM and multi-scale approach, addressing in a direct way the stress resultant plus bending nonlinear hysteretic behaviour of RC plates. The constitutive model devoted to the collapse of RC plates under fast dynamical conditions (Koechlin and Potapov, 2007) can be quoted; however, this model is not appropriate for seismic loading computations. A first attempt meeting the needs of the applications considered for our study was proposed by Markovic et al. (2007), but limited to the only elastic continuum scalar damage of RC plates under cyclic loading conditions, and not accounting for other types of energy dissipation.

1.3. Outline of this work

The aim of the work presented in this paper is to justify the formulation of a stress resultant plus bending cyclic constitutive model for RC slabs and walls, in view of building seismic analyses. This model must account for period elongation of RC buildings due to cracking during earthquake ground motion, and energy dissipation evaluation, needed to assess an equivalent damping effect, in case of low and intermediate seismic ground shaking levels (seen with respect to the load carrying capacity of the building).

One of our aims is then to enlarge the approach presented by Markovic et al. (2007), namely by introducing steel–concrete debonding effect, membrane-bending coupling and accounting for any type of double steel-rebar grid in the thickness of the RC section. Another aim is to build a better justification of model equations: in particular to introduce RC panel section modeling by means of a control volume or "REV" (for representative elementary volume) within a micro–macro approach. In this multi-scale context, a justification of the modeling by means of an averaging homogenisation technique is chosen to deduce, in such way, the overall behaviour of the RC section from local phenomena. Indeed, thanks to the contribution of steel rebar, a positive post-elastic slope can be a priori considered within the global resultant behaviour, avoiding thereby well-known localisation issues as we do not consider, in the analysis, the collapse of the RC section, see Pijaudier-Cabot and Bažant (1987) and Badel et al. (2007). This assumption can be justified by experimental evidence, as quoted by Alliche and Dumontet (2011) and Feenstra and De Borst (1995).

Due to the static indeterminacy of the concrete-steel assembly in the RC section, it is expected that accounting for progressive degradation of both concrete stiffness by cracking and bond at the concrete/steel interface, will be sufficient to describe the complex hysteretic behaviour of RC section, by means of a two-scales approach, justifying the overall behaviour by a schematic description at the fine scale. As a consequence of physical phenomena to be addressed, see §1.1, there is a need for two types of dissipative internal state variables: damage variables and residual strain ones.

In the sense of the categorisation presented at Section 1.2, the proposed model belongs to the homogenised models for RC structural elements, within the GSM framework for nonlinear irreversible behaviour constitutive relations.

The paper is organised as follow: in a first part, the three-dimensional formulation of the concerned periodic homogenisation problem is presented and the proposed constitutive model, coupling damage and debonding is set up. This problem is then analytically solved in one dimension and the closed form of the one-dimensional model is presented. Then, an equivalent rheological modeling is proposed as a physical interpretation of the previously set one-dimensional model. Finally, typical behaviour of the one-dimensional model is studied including parameters influence and the model is applied on an engineering application: the SAFE experimental tests that were conducted at the Joint Research Centre at Ispra, Italy (Pegon et al., 1998) on shear RC walls, see also (Brun et al., 2010).

2. General formulation by Periodic homogenisation

Considering the particular context of the study, a simplified periodic cell is defined and an averaging periodic homogenisation approach for heterogeneous plates is implemented. Variational form of the auxiliary problem is set up and homogenised free Helmholtz energy as well as intrinsic mechanical dissipation are presented. Finally, the macroscopic homogenised constitutive
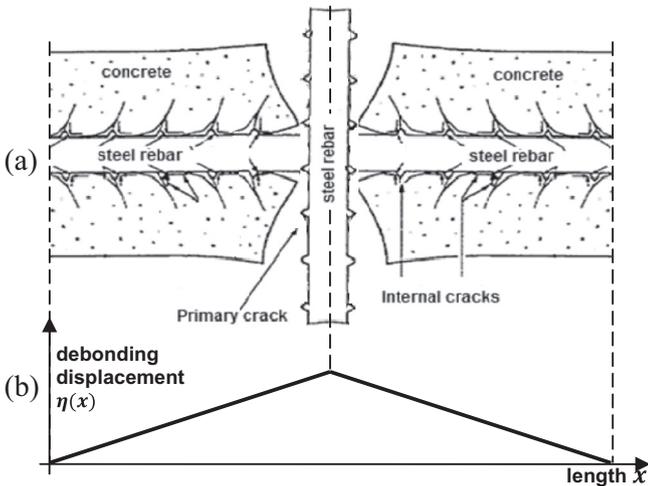
Fig. 2-1. (a) Debonding phenomena at concrete-steel rebar interface (Goto, 1971) (b) Assumed debonding displacement distribution at the interface.

model formulated within the framework of the GSM theory (Halphen and Nguyen, 1975) is proposed.

2.1. From reality to the studied periodic cell

As cyclic loading and seismic solicitations far from collapse are addressed, see Section 1.3, steel is considered as an elastic material whereas concrete is considered as an elastic and damageable material. Concrete can slide down longitudinal steel rebar of the rebar grid beyond a certain threshold.

As shown on Fig. 2-1 (a), the debonding is considered as being maximal at transverse primary-cracks in concrete, frequently initiated by steel rebar being orthogonal to the debonding direction, that is to say orthogonal grid rebar. Indeed, the Young's moduli contrast between concrete and steel induces stress concentration near the steel–concrete interface, and the structural effect of the grid localises this concentration at the grid corner. Moreover, experimental observations by Pascu (1995) clearly show that, during bending experiments on RC plates, the crack pattern matches the position of the grid rebar, underlying the importance of steel reinforcement in crack initiation.

Thus, in the presented study, debonding is considered as periodic with a period equal to the distance between two consecutive
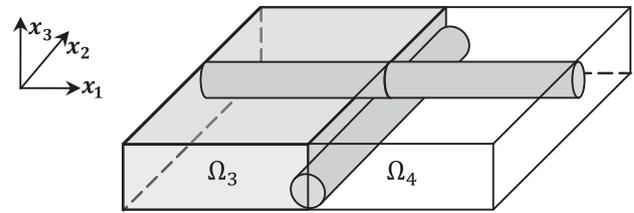

Fig. 2-3. Detail of the layer $\Omega_3 \cup \Omega_4$ including concrete and steel grid.

transverse primary-cracks or/and reinforcing bars of the steel grid perpendicular to the debonding direction. Moreover, the concrete-steel interface behaviour is considered as whether perfectly stick whether perfectly debonding, according the distribution shown on Fig. 2-1(b), consistent with the assumptions proned by Marti et al. (1998) and Pimentel et al. (2010).

Periodic plate homogenisation will be conducted on the periodic cell presented on Fig. 2-2, the thickness of which, H, being the one of the RC plate, with periodicity along x_1 and x_2 directions. Regarding usual RC plates, the ratio between the periodic cell lateral dimensions, l_1 and l_2, and the entire RC plate ones, L_1 and L_2, is about the same order as the ratio between the plate thickness H and its lateral dimensions, l_1 and l_2, and both are small. The effective model is then given by the simultaneous asymptotic limit of these ratios resulting in a Love–Kirchhoff plate model (Caillerie, 1984).

In the following, a double steel grid RC plate is considered. (X_1, X_2) defines the RC plate tangent plane, while X_3 is the normal vector to this tangent plane. The periodic cell can come down to a multi-layer material constituted by a layer $\Omega_1 \cup \Omega_2$ of plain concrete and a layer $\Omega_3 \cup \Omega_4$ including both concrete and steel grid (see Fig. 2-3), alternatively repeated in the plate thickness (see Fig. 2-2). Upper and lower faces are free of charge. The Γ_2 interface, separating Ω_1 from Ω_2 as well as Ω_3 from Ω_4, corresponds to the maximal value of the debonding displacement as presented in Fig. 2-1 (b). Moreover, debonding is occurring both in X_1 and X_2 directions on the multiple Γ_1 interface. For the time being, we restrict our analysis to the stress-resultant (membrane) behaviour without bending; hence debonding is considered as equal on each Γ_1 interface.

Finally, in order to represent concrete damage, it is considered that the concrete layer is constituted of two distinct domains Ω_1 and Ω_2, with two different states of damage for concrete. Indeed, the actual state of damage for concrete in the studied plate is non
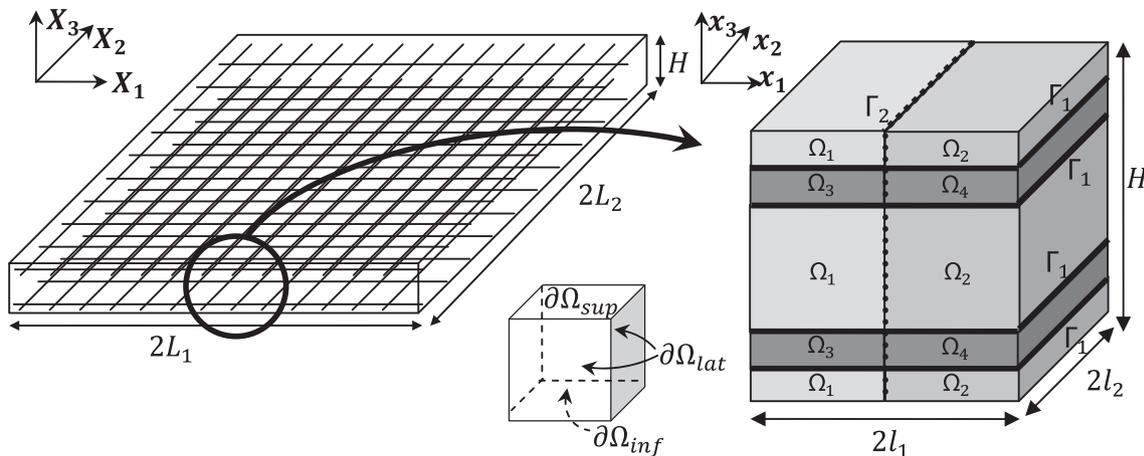

Fig. 2-2. Definition of the considered periodic cell from the real RC plate.

uniform in the concrete volume. As shown in Suquet (1982), keeping the whole generality of the damage local state would result in an infinite number of macroscopic internal variables after the homogenisation process, excluding the possibility to build a practicable Generalised Standard macroscopic model from the microscopic ones. However, Suquet also shown that the number of internal variables can be come down to a finite number if the microscopic internal variables are chosen (or proved to be) piecewise. As a consequence, a piecewise microscopic damage field d is so defined within the whole periodic cell and two values of damage for concrete are chosen. Following the same idea, debonding distribution will be described by only one internal variable, uniform in the whole periodic cell. Thus, the macroscopic and microscopic internal variables (damage and debonding) are identical, thanks to the simple field averaging on the periodic unit cell, and the GSM properties of the macroscopic model are insured.

One might notice that debonding as well as microscopic damage distribution and evolution should be a result of mechanical energy minimisation and not an assumed data of the elastic cell problem. However, these fields depend on the whole RC structure loading history so that microscopic cell non linear equilibrium should be solved for each time increment of global loading. Yet, the aim of our study is to build a macroscopic constitutive model from an a priori homogenisation process. Therefore, the debonding at the interface Γ_1 is considered as assumed and identical for each loading pattern and damage repartition is considered as uniform. Thus, an approximated macroscopic constitutive model is built, depending on the assumed debonding function and the damage distribution used to compute homogenisation stages.

2.2. Membrane cellular homogenisation problem

<u>Notations</u>: The indices of tensor components specify the dimension: latin indices (i,j,k = 1,2,3) denote 3D-space tensors while Greek ones (α,β = 1,2) denote tensors in the plate tangent plane.

In this section the problem considered on the periodic cell (also called "unit cell" due to the periodicity) shown on Fig. 2-2 will be set. The effective constitutive plate model resulting from the periodic plate homogenisation process, and formulated within the framework of GSM (Halphen and Nguyen, 1975) and asymptotic plate (Caillerie, 1984) theories, will be presented using the averaging method (Sanchez-Palencia et al., 1987). Indeed, following these authors, the macroscopic model resulting from averaging homogenisation method is the same as the limit model obtained by the asymptotic approach, assuming elasticity and given anelastic strains. Then, it is assumed (see the proof given in the two previously quoted papers) that, at the macroscopic scale, the state variables are the membrane strain tensor E (for the moment, we do not consider bending), and internal state variables D and E^η, which will be defined from the microscopic state variables: the three-dimensional strain tensor ε, the piecewise damage variable d, the debonding tangential displacement discontinuity on Γ_1 denoted by the function $\eta(x)$ (see Fig. 2-1(b)), all fields being defined within the unit cell.

Regarding periodic homogenisation method, both stress and strain approaches are equivalent (Suquet, 1993); as a consequence, strain approach will be developed with a macroscopic membrane strain tensor E applied on the whole unit cell, E being defined only in the (O,X_1,X_2) macroscopic tangent plane and related to the microscopic strain tensor ε by the averaging of the plan components:

$$E_{\alpha\beta} = \frac{1}{|\Omega|}\int_{\cup\Omega_i}\varepsilon_{\alpha\beta}(u)d\Omega \tag{2-1}$$

The damaged concrete in Ω_2 domain is represented by a damaged elastic stiffness tensor $\mathbb{a}^2(d)$ depending on the microscopic damage variable field d considered as piecewise in this domain. Elastic stiffness tensors $\mathbb{a}^1,\mathbb{a}^3$ and $\mathbb{a}^4$ represent the sound concrete in Ω_1 domain and the steel grid plus concrete in Ω_3 and Ω_4 domains, respectively. The debonding on the Γ_1 interface, is considered as equal to an assumed function η of the (O,x_1,x_2) microscopic plane, depending on the microscopic variables x_1 and x_2. On both interfaces Γ_1 and Γ_2, the following notations are adopted for displacement:

$$u = u_T + u_N.n \tag{2-2}$$

where n is a fixed normal vector to the interface surface.

The macroscopic debonding strain E^η is defined as the average of debonding displacement on the interface Γ_1:

$$E^\eta = \frac{1}{|\Omega|}\int_{\Gamma_1}[\![u_T]\!]\otimes^s x_3 dS \tag{2-3}$$

where $\otimes^s$ denotes the symmetrised tensorial dyadic product and where u is the displacement solution of the problem (2-4) and $[\![\cdot]\!]$ stands for the jump operator on any interface Γ: $[\![v]\!] = \lim_{x\to\Gamma^+}v(x) - \lim_{x\to\Gamma^-}v(x)$.

Moreover, the debonding displacement distribution η is prescribed on Γ_1 interface, so that $E^\eta = \frac{1}{|\Omega|}\int_{\Gamma_1}\eta(x_1,x_2)\otimes^s x_3 dS$. As a consequence, the only non-vanishing components of the macroscopic debonding strain E^η are the $E^\eta_{\alpha3}$. Therefore, E^η is a first-order tensor of the tangent plane which component will be noted E^η_α.

Then, the following elastic mechanical problems in membrane have to be solved on the periodic cell presented on Fig. 2-2, with assumed internal microscopic variables d and $\eta(x)$, and mean membrane strain over the unit cell $E_{\alpha\beta}$:

Find (σ,u) regular enough such as :

$$\begin{cases} div\sigma(u) = 0 & \text{in } \Omega_i \\ \sigma(u) = \mathbb{a}^i(d):\varepsilon(u) & \text{in } \Omega_i \\ \varepsilon(u)\text{periodic} & \text{on } \partial\Omega_{lat} \\ \sigma(u).n \text{ antiperiodic} & \text{on } \partial\Omega_{lat} \\ \sigma.n = 0 & \text{on } \partial\Omega_{sup} \text{ and } \partial\Omega_{inf} \\ [\![\sigma]\!]\cdot n = 0 & \text{on } \Gamma_2 \\ [\![u]\!] = 0 & \text{on } \Gamma_2 \\ [\![\sigma]\!]\cdot n = 0 & \text{on } \Gamma_1 \\ [\![u_N]\!] = 0 & \text{on } \Gamma_1 \\ [\![u_T]\!] = \eta(x) & \text{on } \Gamma_1 \\ \varepsilon(u) = 1/2(^t grad(u) + grad(u)) & \text{in}\Omega_i \\ \langle\varepsilon_{\alpha\beta}(u)\rangle_\Omega = E_{\alpha\beta} \end{cases} \tag{2-4}$$

where $\langle\cdot\rangle_\Omega = \frac{1}{|\Omega|}\int_{\cup\Omega_i}\cdot d\Omega$ stands for the average value of the considered field on the periodic cell. Usual regularity assumptions are adopted for (σ,u).

The local problem (2-4) can be cut down to five problems concerning auxiliary periodic displacement fields denoted by χ, called the auxiliary problems, through the following decomposition in Ω (Andrieux et al., 1986; Sanchez-Palencia, 1980):

$$u_\alpha(x) = E_{\alpha\beta}x_\beta + E_{\beta\gamma}\chi^{\beta\gamma}_\alpha(x) + E^\eta_\beta\chi^{\eta\beta}_\alpha(x) \text{ and } u_3(x)$$
$$= E_{\beta\gamma}\chi^{\beta\gamma}_3(x) + E^\eta_\beta\chi^{\eta\beta}_3(x) \tag{2-5}$$

$E_{\alpha\beta}$ is then the mean strain over the unit cell, $\chi^{\beta\gamma}$ is the auxiliary periodic displacement field resulting from the application of a unitary mean strain $E_{\beta\gamma}$ over the unit cell and $\chi^{\eta\beta}$ is the auxiliary displacement field resulting from the application of a unitary macroscopic debonding strain E^η_β over the unit cell.

Finally, the following variational form of the auxiliary problems is then set up for assumed unitary membrane strain tensor $E_{\alpha\beta}$, normalised debonding function $\hat{\eta}_\alpha(x_\alpha)$, and damage distribution d:

Find $\boldsymbol{\chi}^{\alpha\beta} \in \mathcal{U}_{ad}^0$ such as :

$$\int_{\cup\Omega_i} \varepsilon_{pq}(\boldsymbol{\chi}^{\alpha\beta})\mathbb{a}_{pqrs}^i(d)\varepsilon_{rs}(\boldsymbol{v})d\Omega = -\int_{\cup\Omega_i} \mathbb{a}_{\alpha\beta rs}^i(d)\varepsilon_{rs}(\boldsymbol{v})d\Omega \quad \forall \boldsymbol{v} \in \mathcal{U}_{ad}^0$$

Find $\boldsymbol{\chi}^{\eta\alpha} \in \mathcal{U}_{ad}^\alpha$ such as :

$$\int_{\cup\Omega_i} \varepsilon_{pq}(\boldsymbol{\chi}^{\eta\alpha})\mathbb{a}_{pqrs}^i(d)\varepsilon_{rs}(\boldsymbol{v} - \boldsymbol{\chi}^{\eta\alpha})d\Omega = 0 \quad \forall \boldsymbol{v} \in \mathcal{U}_{ad}^\alpha$$

$$(2\text{-}6)$$

where $\mathcal{U}_{ad}^0 = \{\boldsymbol{v} \text{ regular, periodic on } \partial\Omega_{lat}, \text{continuous in } \Omega\}$ and $\mathcal{U}_{ad}^\alpha = \{\boldsymbol{v} \text{ regular, periodic on } \partial\Omega_{lat}, [\![v_N]\!] = 0 \text{ and } [\![\boldsymbol{v_T}]\!] = \hat{\eta}_\alpha \quad (x_\alpha)$ on $\Gamma_1\}$ where the normalised debonding function $\hat{\eta}_\alpha(x_\alpha)$ is defined as $\eta_\alpha(x_\alpha) = E_\alpha^\eta.\hat{\eta}_\alpha(x_\alpha)$. Usual regularity assumptions are adopted for the two functional spaces $\mathcal{U}_{ad}^0$ and $\mathcal{U}_{ad}^\alpha$.

Even though the auxiliary problems (2-6) could contain non-linearity through internal state variables, they remain linear as long as these internal variables are assumed to have an assigned value, which is the situation in our study.

The assumed debonding function $\eta_\alpha(x_\alpha)$ can have any distribution as long as it is assigned and identical for each loading pattern. An example of a debonding function is presented in Fig. 2-1 (b). Authors will justify in Section 3 that this particular distribution of debonding is consistent with the one-dimensional damage debonding problem. More generally, this is also consistent with usual assumptions on bond-stress distribution presented, for instance, by Marti et al. (1998).

2.3. Homogenised constitutive model

The homogenisation procedure used in the following lies on the assimilation property of the asymptotic boundary values problem at macroscopic scale with the averaged problem on the unit cell through the extended Hill-Mandel mechanical principle (Hill, 1972; Sanchez-Palencia et al., 1987; Suquet, 1993). The balance equations written at the microscopic scale ensure the relation between macroscopic stress resultant Σ and microscopic stress field $\boldsymbol{\sigma}$. Thanks to the decomposition (2-5), the microscopic strain becomes:

$$\boldsymbol{\varepsilon}(\boldsymbol{u}) = \boldsymbol{E} + E_{\beta\gamma}\boldsymbol{\varepsilon}(\boldsymbol{\chi}^{\beta\gamma}) + E_\beta^\eta\boldsymbol{\varepsilon}(\boldsymbol{\chi}^{\eta\beta}) \tag{2-7}$$

So, once the five ($\boldsymbol{\chi}^{\alpha\beta}$ and $\boldsymbol{\chi}^{\eta\alpha}$) independent linear elastic auxiliary problems (2-6) solved (e.g. by FEM), the homogenised free Helmholtz energy surface density is given by:

$$2\mathcal{W}(\boldsymbol{E}, D, \boldsymbol{E^\eta}) = \langle\langle\boldsymbol{\varepsilon}(\boldsymbol{u}) : \mathbb{a}(d) : \boldsymbol{\varepsilon}(\boldsymbol{u})\rangle\rangle_\Omega = \boldsymbol{E} : \langle\langle\mathbb{a}(d)_\Omega$$
$$: \boldsymbol{E} - E_{\alpha\beta}\boldsymbol{\varepsilon}(\boldsymbol{\chi}^{\alpha\beta}) : \mathbb{a}(d) : \boldsymbol{\varepsilon}(\boldsymbol{\chi}^{\gamma\delta})\rangle\rangle_\Omega E_{\gamma\delta} + 2\boldsymbol{E}$$
$$: \langle\langle\mathbb{a}(d) : \boldsymbol{\varepsilon}(\boldsymbol{\chi}^{\eta\gamma})\rangle\rangle_\Omega E_\gamma^\eta + E_\alpha^\eta\langle\langle\boldsymbol{\varepsilon}(\boldsymbol{\chi}^{\eta\alpha}) : \mathbb{a}(d)$$
$$: \boldsymbol{\varepsilon}(\boldsymbol{\chi}^{\eta\gamma})\rangle\rangle_\Omega E_\gamma^\eta = \boldsymbol{E} : \mathbb{A}(D) : \boldsymbol{E} + 2\boldsymbol{E} : \mathbb{B}(D)$$
$$: \boldsymbol{E^\eta} + \boldsymbol{E^\eta} : \mathbb{C}(D) : \boldsymbol{E^\eta} \tag{2-8}$$

where $\langle\langle\cdot\rangle\rangle_\Omega = \frac{H}{|\Omega|}\int_{\cup\Omega_i} \cdot d\Omega$ stands for the average value of the considered field on the periodic cell time its height H, and $\mathbb{A}, \mathbb{B}, \mathbb{C}$ are homogenised symmetric fourth, third and second order tensors of the tangent plane, respectively, defined by:

$$\mathbb{A}_{\alpha\beta\gamma\delta}(D) = \langle\langle\mathbb{a}_{\alpha\beta\gamma\delta}(d)\rangle\rangle_\Omega + \langle\langle\boldsymbol{\varepsilon}(\boldsymbol{\chi}^{\alpha\beta}) : \mathbb{a}(d) : \boldsymbol{\varepsilon}(\boldsymbol{\chi}^{\gamma\delta})\rangle\rangle_\Omega$$
$$\mathbb{B}_{\alpha\beta\gamma}(D) = \langle\langle\mathbb{a}_{\alpha\beta ij}(d)\varepsilon_{ij}(\boldsymbol{\chi}^{\eta\gamma})\rangle\rangle_\Omega$$
$$\mathbb{C}_{\alpha\gamma}(D) = \langle\langle\boldsymbol{\varepsilon}(\boldsymbol{\chi}^{\eta\alpha}) : \mathbb{a}(d) : \boldsymbol{\varepsilon}(\boldsymbol{\chi}^{\eta\gamma})\rangle\rangle_\Omega$$

The stress resultant differentiated from this free energy density reads then:

$$\Sigma = \frac{\partial W}{\partial \boldsymbol{E}} = \mathbb{A}(D) : \boldsymbol{E} + \mathbb{B}(D) : \boldsymbol{E^\eta} \tag{2-9}$$

We observe that this free energy density introduces a damage-dependent anelastic strain, unlike many usual expressions as in Chaboche (2003) or Nedjar (2001), Shao et al. (2006) but similar to expressions from Andrieux et al. (1986).

According to the thermodynamics of irreversible processes, the free energy density (2-8) can be differentiated to get the following thermodynamical forces (debonding stress and energy restitution rate):

$$\Sigma^\eta = -\frac{\partial W}{\partial \boldsymbol{E}^\eta}; \quad G = -\frac{\partial W}{\partial D} \tag{2-10}$$

Finally, once the elastic cellular problem solved and the free Helmholtz energy set up, the overall internal variables evolution has to be dealt. First of all, microscopic dissipative laws have to be defined. We will consider dissipation processes as simple as possible (constant thresholds parameters (k_0, σ_{crit}), no hardening ...) and microscopic GSM models with the following threshold functions for damage and debonding, respectively (g being the microscopic energy restitution rate for damaged concrete of domain Ω_2 and $\sigma_{\alpha3}$ being the tangential components of the stress vector $\boldsymbol{\sigma.n}$ on the interface Γ_1):

$$f_d(g) = g - k_0 \leqslant 0 \text{ and } f_\eta^\alpha(\sigma_{\alpha3}) = \sigma_{\alpha3}^2 - \sigma_{crit}^2 \tag{2-11}$$

Microscopic associated flow rules are so written as:

$$\dot{d} = \dot{\lambda}_d \frac{\partial f_d(g)}{\partial g} \text{ and } [\![\dot{u}]\!]_\alpha = \dot{\lambda}_\eta^\alpha \frac{\partial f_\eta^\alpha(\sigma_{\alpha3})}{\partial\sigma_{\alpha3}} \tag{2-12}$$

where $\dot{\lambda}_d$ and $\dot{\lambda}_\eta^\alpha$ are positive scalars.

Regarding the work of Stolz (2010) on interfaces and according to the theory developed by Suquet (1993), macroscopic intrinsic mechanical dissipation is built as follows:

$$\mathcal{D}(\dot{D}, \dot{\boldsymbol{E}}^\eta) = \langle\langle\boldsymbol{\sigma} : \dot{\boldsymbol{\varepsilon}}\rangle\rangle_\Omega - \langle\langle w_{,\varepsilon} : \dot{\boldsymbol{\varepsilon}} + w_{,d}\dot{d}\rangle\rangle_\Omega - \frac{H}{|\Omega|}\int_{\Gamma_1} w_{,\eta}\dot{\eta}dS$$
$$= G\dot{D} + \boldsymbol{\Sigma^\eta} \cdot \dot{\boldsymbol{E}}^\eta \tag{2-13}$$

where $w(\boldsymbol{\varepsilon},\boldsymbol{\eta},d)$ denotes the microscopic free Helmholtz energy density for each material constituting the unit cell.

As a consequence, macroscopic threshold functions are identified from the macroscopic intrinsic mechanical dissipation as:

$$f_d(G) = G - Hk_0 \leqslant 0 \text{ and } f_\eta^\alpha(\Sigma_{\alpha3}^\eta) = (\Sigma_{\alpha3}^\eta)^2 - H^2\sigma_{crit}^2 \leqslant 0 \tag{2-14}$$

At last, the macroscopic evolution laws take the form of normality rules:

$$\dot{D} = \dot{\lambda}_d \frac{\partial f_d(G)}{\partial G} \text{ and } \dot{E}_{\alpha3}^\eta = \dot{\lambda}_\eta^\alpha \frac{\partial f_\eta^\alpha(\Sigma_{\alpha3}^\eta)}{\partial\Sigma_{\alpha3}^\eta} \tag{2-15}$$

where $\dot{\lambda}_d$ and $\dot{\lambda}_\eta^\alpha$ are positive scalars.

The two functions $\mathcal{W}$ – the free Helmholtz energy density – and $\mathcal{D}$ – the macroscopic intrinsic mechanical dissipation, from which can be defined the dissipation potential – define the effective macroscopic constitutive model of the homogenised material, which is formulated within the framework of the GSM theory. This macroscopic constitutive model comprises only two internal state variables D and $\boldsymbol{E}^\eta$, given the fact that is assumed that microscopic damage d is piecewise, and $\boldsymbol{E}^\eta$ is defined as an average of the debonding function $\boldsymbol{\eta}$, on the whole unit cell. Of course, even if the free energy density presented in Eq. (2-8) has a quite general expression, the values of $\mathbb{A}, \mathbb{B}, \mathbb{C}$ tensor components are closely depending on the assumed microscopic damage field in the unit cell and the debonding distribution at the Γ_1 interface.

3. Closed-form solution of the cellular problem in one dimension

Considering the homogenisation approach presented previously, a constitutive model for RC beams under tensile-compressive loading conditions, coupling damage and debonding is built based on an analytical solution of the cellular problem in one dimension. Thanks to this analytical solution, original macroscopic free energy and dissipation potential, coupling damage and debonding, are sorted out. This one dimensional homogenisation is then re-interpreted through an equivalent rheological model that allows us to define a very simple approach of homogenisation. Thus, the so-built well defined closed-form model exhibits easy-to-determine properties.

3.1. One dimensional simplifications and hypothesis

Considering a one dimensional approach, the unit cell presented in Fig. 2-2 can come down to the one proposed in Fig. 3-1. The preferred dimension for this study will be the x_1 axis.

In one dimension, the Poisson's coefficient is assumed equal to zero, hence microscopic stiffness tensors $\mathbb{a}^i$ are reduced to the Young's moduli of each considered material noted a^i. It will be considered that the Young's modulus of Ω_2 domain depends on the internal damage variable d as follows: $a^2(d) = a^2 \zeta(d)$; ζ being an assumed decreasing convex damage function of C^2 class. Finally, considering one dimensional auxiliary displacement fields χ_1^{11} for elasticity and $\chi_1^{\eta 1}$ for debonding, only dependent on the x_1 variable, the five independent auxiliary problems presented in (2-6) can be simplified to only two auxiliary problems:

The elastic auxiliary problem

Find $\chi_1^{11} \in \mathcal{U}_{ad}^0$ such as :

$$\int_{\cup \Omega_i} \chi_{1,1}^{11} a^i(d) v_{1,1} d\Omega = - \int_{\cup \Omega_i} a^i(d) v_{1,1} d\Omega \quad \forall v_1 \in \mathcal{U}_{ad}^0 \tag{3-1}$$

where
$\mathcal{U}_{ad}^0 = \{ v_1 \text{ regular}/v_1 \text{ periodic on} - l_1 \text{ and } l_1, [\![v_1]\!] = 0 \text{ on } \Gamma_1 \}$

The debonding auxiliary problem:

Find $\chi_1^{\eta 1} \in \mathcal{U}_{ad}^1$ such as :

$$\int_{\cup \Omega_i} a^i(d) \chi_{1,1}^{\eta 1} (v_{1,1} - \chi_{1,1}^{\eta 1}) d\Omega = 0 \quad \forall v_1 \in \mathcal{U}_{ad}^1 \tag{3-2}$$

where
$\mathcal{U}_{ad}^1 = \{ v_1 \text{regular}/v_1 \text{ periodic on} - l_1 \text{ and } l_1, [\![v_1]\!] = \hat{\eta}_1(x_1) \text{ on } \Gamma_1 \}$
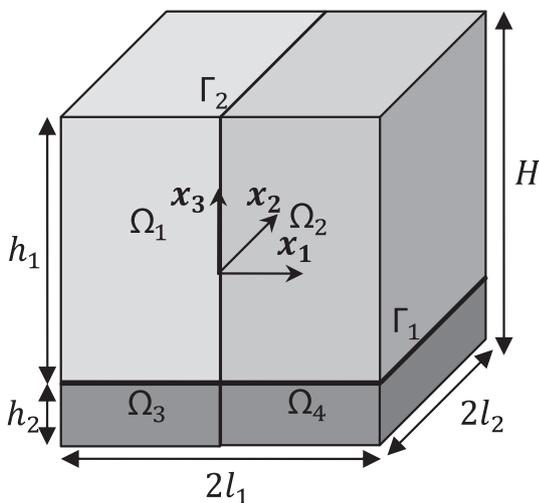

Fig. 3-1. Definition of the one dimensional periodic unit cell.

In this section, the normalised debonding function $\hat{\eta}_1$ is considered as assigned but with an unknown distribution.

Moreover, according to (2-11), two microscopic threshold functions – one for each dissipative variable – are assumed. They are chosen to be as simple as possible, without any hardening and with a constant threshold parameter k_0 for damage and σ_{crit} for debonding:

$$f_d = g - k_0 \quad \text{and} \quad f_\eta = \sigma_1^{\eta 2} - \sigma_{crit}^2 \leqslant 0 \tag{3-3}$$

where $g = \frac{-1}{2} a^2 \zeta'(d) \chi_{1,1}^2$ is the energy restitution rate for the microscopic damage model of Ω_2 domain. Prime ($\cdot'$) stands for the standard derivation of function with one variable.

Microscopic associated flow rules are then written as:

$$\dot{d} = \dot{\lambda}_d \frac{\partial f_d(g)}{\partial g} \quad \text{and} \quad [\![\dot{u}_1]\!] = \dot{\lambda}_\eta \frac{\partial f_\eta(\sigma_1^\eta)}{\partial \sigma_1^\eta} \tag{3-4}$$

where $\dot{\lambda}_d$ and $\dot{\lambda}_\eta$ are positive scalars.

This particular choice of threshold functions can be discussed but appears to be the simplest one for the present study. In order to improve the model, more sophisticated microscopic threshold functions can be chosen if desired, but authors wish to underline that they often induce additional parameters difficult to apprehend for engineers.

3.2. Homogenised one dimensional damage-debonding coupled model

Considering that Ω_1 and Ω_2 domains are filled with sound and damaged concrete, respectively, and that Ω_3 and Ω_4 domains are filled with the same steel, the following notations for Young's moduli will be adopted: $a^1 = a^c, a^2 = a^c \zeta(d), a^3 = a^s = a^4$. The two superscripts c and s denote the "concrete" and "steel", respectively.

A judicious choice of trial functions v_1 in the two auxiliary problems (3-1) and (3-2) leads to $\chi_{1,11}^{11} = 0$ and $\chi_{1,11}^{\eta 1} = 0$ in each domain Ω_i. Therefore, microscopic strain is constant in each domain Ω_i and noted ε^i. To be consistent with this distribution of microscopic strain, the normalised debonding function $\hat{\eta}_1$ has to be bilinear and periodic, so it is defined by:

$$\eta_1(x_1) = \begin{cases} E_{13}^\eta (l_1 + x_1) & \forall x_1 \in [-l_1; 0] \\ E_{13}^\eta (l_1 - x_1) & \forall x_1 \in [0; l_1] \end{cases} \tag{3-5}$$

So the distribution of microscopic debonding function corresponds to the one of the debonding displacement presented in Fig. 2-1 (b).

Then the two auxiliary problems (3-1) and (3-2) can be solved in a closed-form and lead to the following auxiliary displacement fields.

Elastic auxiliary displacement field:

$$\chi_{1,1}^{11} = \begin{cases} E_{11} \dfrac{a^c h_1(\zeta(d) - 1)}{2a^s h_2 + a^c h_1(1 + \zeta(d))} & \text{in } \Omega_1 \\ -\varepsilon_{11}^1 & \text{in } \Omega_2 \\ \varepsilon_{11}^1 & \text{in } \Omega_3 \\ -\varepsilon_{11}^1 & \text{in } \Omega_4 \end{cases} \tag{3-6}$$

Debonding auxiliary displacement field:

$$\chi_{1,1}^{\eta 1} = \begin{cases} -E_1^\eta \dfrac{2a^s h_2}{2a^s h_2 + a^c h_1(1 + \zeta(d))} & \text{in } \Omega_1 \\ -\varepsilon_{11}^1 & \text{in } \Omega_2 \\ E_1^\eta \dfrac{a^c h_1(1 + \zeta(d))}{2a^s h_2 + a^c h_1(1 + \zeta(d))} & \text{in } \Omega_3 \\ -\varepsilon_{11}^3 & \text{in } \Omega_4 \end{cases} \tag{3-7}$$

Once the auxiliary fields expressions are set up, it is then possible to express analytically the macroscopic Helmholtz free energy density from (2-8):

$$2\mathcal{W}(E,D,E^\eta) = A(D)E_{11}^2 + 2B(D)E_{11}E_1^\eta + C(D)E_1^{\eta^2} \qquad (3\text{-}8)$$

where A, B and C are homogenised factors explicitly expressed as a function of Young's moduli a^c and a^s, height of concrete domain h_1, height of steel domain h_2 and damage function ζ:

$$A(D) = \frac{(a^s h_2 + a^c h_1)(a^s h_2 + a^c h_1 \zeta(D))}{2a^s h_2 + a^c h_1(1 + \zeta(D))} \qquad (3\text{-}9)$$

$$B(D) = \frac{a^s h_2 a^c h_1(\zeta(D) - 1)}{2a^s h_2 + a^c h_1(1 + \zeta(D))} \qquad (3\text{-}10)$$

$$C(D) = \frac{a^s h_2 a^c h_1(1 + \zeta(D))}{2a^s h_2 + a^c h_1(1 + \zeta(D))} \qquad (3\text{-}11)$$

It can be underlined that, given this expression of $B(D)$, there is no coupling between elasticity and debonding until damage takes non zero values. Indeed, if $D = 0$, then $\zeta(D) = 1$ and $B(D) = 0$.

From this macroscopic Helmholtz free energy density (3-8), the following thermodynamic forces, stress Σ, debonding stress Σ^η and energy restitution rate G can be derived:

$$\Sigma = \frac{\partial \mathcal{W}}{\partial E_{11}} = \frac{(a^s h_2 + a^c h_1)(a^s h_2 + a^c h_1 \zeta(D))}{2a^s h_2 + a^c h_1(1 + \zeta(D))} E_{11} + \frac{a^s h_2 a^c h_1(\zeta(D) - 1)}{2a^s h_2 + a^c h_1(1 + \zeta(D))} E_1^\eta \qquad (3\text{-}12)$$

$$\Sigma^\eta = -\frac{\partial \mathcal{W}}{\partial E^\eta} = -\frac{a^s h_2 a^c h_1(\zeta(D) - 1)}{2a^s h_2 + a^c h_1(1 + \zeta(D))} E_{11} - \frac{a^s h_2 a^c h_1(1 + \zeta(D))}{2a^s h_2 + a^c h_1(1 + \zeta(D))} E_1^\eta \qquad (3\text{-}13)$$

$$G = -\frac{\partial \mathcal{W}}{\partial D} = \frac{-a^c h_1 \zeta'(D)}{2} \left[\frac{(a^s h_2 + a^c h_1)E_{11} + 2a^s h_2 E_1^\eta}{2a^s h_2 + a^c h_1(1 + \zeta(D))} \right]^2 \qquad (3\text{-}14)$$

The macroscopic debonding threshold function f_η remains unchanged:

$$f_\eta = \Sigma_1^{\eta^2} - H^2 \sigma_{crit}^2 \leqslant 0 \qquad (3\text{-}15)$$

With the help of the closed form solutions presented in (3-6) and (3-7), it is possible to rewrite the damage threshold function f_d as a function of macroscopic strain E_{11} and macroscopic internal variables D and E_{13}^η:

$$f_d(G) = \frac{-a^c h_1 \zeta'(D)}{2} \left[\frac{(a^s h_2 + a^c h_1)E_{11} + 2a^s h_2 E_1^\eta}{2a^s h_2 + a^c h_1(1 + \zeta(D))} \right] - H k_0$$
$$= G - H k_0 \qquad (3\text{-}16)$$

Finally, according to (2-15), the intrinsic mechanical dissipation is set up as:

$$\mathcal{D}(\dot{D}, \dot{E}_1^\eta) = G\dot{D} + \Sigma_1^\eta \dot{E}_1^\eta \qquad (3\text{-}17)$$

where G and Σ^η are the associated dual variables of D and E_1^η, respectively.

3.3. Equivalent rheological modeling

In order to provide a simpler perspective of the work presented hereafter, an equivalent rheological modeling is proposed. The rheological approach appears to be an efficient way to explain the microscopic physical mechanisms ruling the homogenised model. Such kind of lumped approach was already used for instance by Amadio and Fragiacomo (1993) to study the specific problem of connections of composite steel–concrete beams. The underlying idea of this rheological model is to explain, in the simplest way and with easily identifiable parameters, the behaviour of the homogenised model representing a RC member subjected to tension or compression in the direction of its steel rebar.

The RC member is considered as an assembly along its thickness of periodic elementary volumes similar to the one presented on Fig. 2-1. The periodicity is based on the periodic distribution of stirrups in RC members. The periodic unit cell is constituted of two
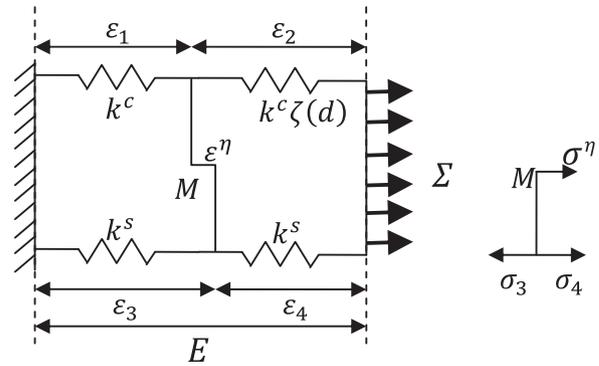

Fig. 3-2. Rheological model representing schematically the unit cell of Fig. 2-2 in one dimension.

main materials (concrete and steel) represented by two springs working in parallel. The concrete-steel bond generating debonding is represented by a sliding pad with a specific threshold located at point M (Fig. 3-2). In order to load this sliding pad, it is necessary to damage only one part of concrete area. Therefore, the springs representing concrete and steel are divided into two springs in series, the sliding pad being localised at the separation, and only one spring of concrete (arbitrary the right-handed one) is damaged. Finally, the following assembly, presented Fig. 3-2, is built, producing a second rank statically indeterminate system of four springs with six links, one of which being a sliding pad.

The study of this simple model is conducted in the way it would be with a periodic homogenisation approach, separating macroscopic variables from microscopic ones, the main goal being to determine macroscopic behaviour from a microscopic description of the system.

The two superscripts c and s denote the "concrete" and "steel" components, respectively. At the macro-scale, the system is controlled by one of the two macroscopic variables E or Σ and at the micro-scale, each spring is defined by its own strain or stress: ε_i or σ_i.

The stiffness of concrete and steel springs (respectively k^c and k^s) are determined directly from the Young's modulus and the proportions of each material: $k^c = a^c h_1$ and $k^c = a^c h_2$. The sliding pad is defined by the debonding amplitude E^η, the debonding stress σ^η and a threshold stress σ_{crit} given by experiments. The damaged stiffness of the right-handed concrete spring $k^c \zeta(d)$ is based on the elastic stiffness k^c multiplied by a decreasing damage function ζ.

The Table 1 summarises all macroscopic and microscopic variables and their associated dual variables. Moreover, there is a need to underline that loading is applied through one of the two macroscopic variables Σ or E while d and ε^η are two assigned internal variables, each one being associated to a dissipative process, damage and debonding, respectively. Those two internal variables are chosen to be piecewise at the microscopic scale and, considering the fact that the present study is conducted in one dimension; the microscopic (d, ε^η) and macroscopic (D, E^η) couples of internal variables have identical values, respectively, so as their associated dual variables (g, σ^η) and (G, Σ^η) have.

The static equilibrium, the macroscopic load Σ being given, reads:

$$\Sigma = \sigma_1 + \sigma_3 = \sigma_2 + \sigma_4; \quad \Sigma^\eta = \sigma^\eta = \sigma_3 - \sigma_4 = \sigma_2 - \sigma_1 \qquad (3\text{-}18)$$

The two compatibility equations give, for the macroscopic strain E and the debonding amplitude E^η:

$$E = \varepsilon_1 + \varepsilon_2 = \varepsilon_3 + \varepsilon_4; \quad E^\eta = \varepsilon^\eta = \varepsilon_3 - \varepsilon_1 = \varepsilon_2 - \varepsilon_4 \qquad (3\text{-}19)$$

Considering these equations, microscopic strain is constant in each spring, imposing a debonding distribution similar to the one

Table 1
State variables of the rheological model.

	Microscopic state variables Internal						Macroscopic state variables internal		
Primal	d	ε^{η}	ε_1	ε_2	ε_3	ε_4	D	E^{η}	E
Associated	g	σ^{η}	σ_1	σ_2	σ_3	σ_4	G	Σ^{η}	Σ

proposed in (3-5) for the one dimensional solution of the homogenisation problem.

The macroscopic mechanical state variables are deduced from the minimisation of the complementary energy of the system shown on Fig. 3-2:

$$\Sigma = \frac{(k^s + k^c)(k^s + k^c \zeta(d))}{2k^s + k^c(1 + \zeta(d))}E + \frac{k^s k^c(\zeta(d) - 1)}{2k^s + k^c(1 + \zeta(d))}E^{\eta} \qquad (3\text{-}20)$$

$$\Sigma^{\eta} = -\frac{k^s k^c(\zeta(d) - 1)}{2k^s + k^c(1 + \zeta(d))}E - \frac{2k^s k^c(1 + \zeta(d))}{2k^s + k^c(1 + \zeta(d))}E^{\eta} \qquad (3\text{-}21)$$

These two thermodynamic forces are the same as the ones corresponding to the one-dimensional cellular problem, see Eqs. (3-12) and (3-13).

The presented rheological model is so equivalent to the one-dimensional solution of the homogenisation problem presented in section (2-6), and provides an easier way to illustrate the general modeling proposed before.

4. Application to reinforced concrete

The previously described problem is generalised and can be applied to whatever heterogeneous material with damageable matrix and periodic internal debonding between matrix and inclusions. In the following section, a range of specific hypotheses for the application to RC is set up and the model typical behaviour is presented. Then parameter identification is explained and a parametric study is conducted.

In this section, for the sake of simplicity, the notations are the one used in the rheological modeling presented in Section 3.3.

4.1. Definition of the microscopic damage model

It is well-known that damaged concrete behaviour under tension loading differs from the one under compression loading, so that a non-symmetrical description of damage has to be introduced. Damage is so defined through a damage function ζ based on the one proposed by Badel et al. (2007), giving a bilinear stress–strain response in damage one dimensional cyclic loading
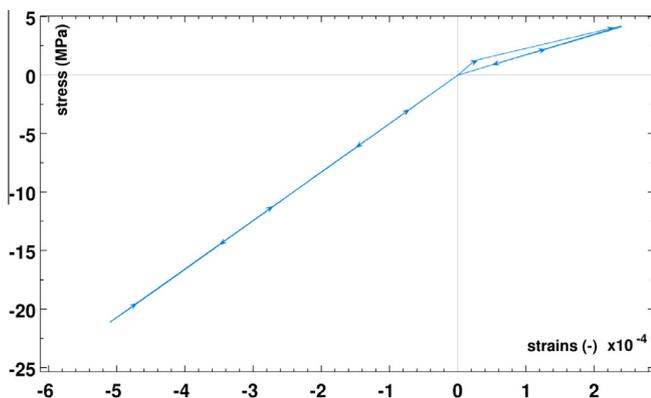
paths as presented in Fig. 4-1. Indeed, the stress rate is given by (4-1) for a damage elastic constitutive relation $\sigma = A\zeta(d)\varepsilon$ and associated flow.

$$\dot{\sigma} = A\dot{\varepsilon}\left(\zeta(d) - \frac{2(\zeta'(d))^2}{\zeta''(d)}\right) \qquad (4\text{-}1)$$

So the ζ function has to be a rational fraction of the polynomials of first order in d to give a bilinear strain–stress response for monotonic loadings.

This dissymmetric damage function addresses the two main physical phenomena governing the concrete response under tension and compression loadings: dissymmetric behaviour under tension and compression loadings as well as stiffness recovery through crack closure.

The closed-form expression of the damage function ζ is the following:

$$\zeta(d) = \frac{1 + \gamma_+ d}{1 + d}H(\varepsilon_2) + \frac{\alpha_- + \gamma_- d}{\alpha_- + d}H(-\varepsilon_2) \qquad (4\text{-}2)$$

where H denotes the Heaviside function, α_- a positive material parameter representing the ratio of compression contribution related to tension one, and where (γ_+, γ_-) are two material parameters representing the asymptotical stiffness alteration for tension and compression, respectively. The stiffness recovery corresponding to crack closure is based on the difference between γ_+ and γ_-.

It should be highlighted that, within the framework of this formulation for the convex decreasing damage function ζ, the damage variable d ranges from 0 to infinite. A qualitative representation of the function ζ is proposed in Fig. 4-2.

One can notice that local damage function ζ is based on Heaviside function of ε_2 variable. Thanks to the closed form expression of ε_2, resulting from the study of the rheological model presented in Section 3.3, it is possible to write ε_2 as a function of the macroscopic strain E and the internal variable E^{η}:

$$\varepsilon_2 = \frac{k^s + k^c}{2k^s + k^c(1 + \zeta(d))}E + \frac{2k^s}{2k^s + k^c(1 + \zeta(d))}E^{\eta} \qquad (4\text{-}3)$$

As a consequence, homogenised factors A, B and C present a dissymmetry based at $\varepsilon_2 = 0$, i.e. $E = \frac{-2k^s}{k^s + k^c}E^{\eta}$ and not $E = 0$. So there is no more an usual and simple tension–compression dissymmetry but a debonding strain dependent one. This will represent the delay due
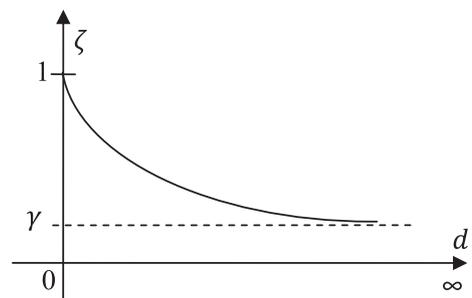

Fig. 4-1. Stress–strain cyclic response of concrete damaged through the damage function ζ.

Fig. 4-2. Qualitative representation of the damage function ζ.

to the closing of the debonding caused by concrete cracks as observed experimentally.

Finally, considering this peculiar damage function, it can be determined that the considered Helmholtz free energy density (3-8) is convex under the following conditions on local material parameters (γ_+, γ_-):

$$\frac{-k^s}{2k^c + k^s} \leqslant \gamma_+, \gamma_- \leqslant 1 \qquad (4\text{-}4)$$

Thanks to these conditions, local damage parameter γ can be negative, producing decreasing concrete stress–strain response and exhibiting local softening behaviour, while homogenised factors A, B and C remain positive, describing macroscopic weakening behaviour without softening. This peculiarity of the model will be quite useful to describe the global behaviour of RC material in tension. Indeed, concrete behaviour is fragile in tension (Reinhardt et al., 1986), so that softening has to be locally considered for concrete behaviour, whereas steel rebar ensures a positive post-elastic slope for the overall RC section.

4.2. Parameters identification

Considering the damage function presented in Section 4.1, and specific threshold functions proposed by (3-3), the homogenised rheological model is parameterised with seven mechanical parameters:

– k^s: elastic modulus of steel times proportion of steel in RC section,
– k^c: elastic modulus of concrete times proportion of concrete in RC section,
– γ_+: damage parameter for concrete under uni-axial tensile loadings related to the asymptotical behaviour of concrete when damage is infinite (a priori: $\gamma_+ \leqslant 0$ to represent concrete softnening behaviour in tension),
– γ_-: damage parameter for concrete under uni-axial compressive loadings related to the asymptotical behaviour of concrete when damage is infinite,
– σ_{d+}: first damage stress threshold for concrete in tension
– σ_{d-}: first damage stress threshold for concrete in compression
– σ_{crit}: first slip threshold for concrete-steel bond

Given those parameters, most of them being easily identified from section geometry and material data (except perhaps σ_{d-} which is less usual), macroscopic threshold constants are determined as follows. As presented in Section 2, macroscopic threshold constants are the same as local ones. So they are determined by local behaviour of components. Therefore, the debonding threshold constant σ_{crit} is the one of already given parameters and the damage threshold constant k_0 is determined by:

$$k_0 = \frac{(1 - \gamma_+)\sigma_{d+}^2}{2k^c} = \frac{(1 - \gamma_-)\sigma_{d-}^2}{2k^c \alpha_-} \qquad (4\text{-}5)$$

where α_- stands for the ratio between tension and compression contributions:

$$\alpha_- = \frac{(1 - \gamma_-)\sigma_{d-}^2}{(1 - \gamma_+)\sigma_{d+}^2} \qquad (4\text{-}6)$$

5. Typical responses and parametric study of the 1D model

The presented one-dimensional global model has been numerically implemented using a fixed-point algorithm and gives useful results in terms of energy dissipation, irreversible strains and shape of hysteretic cycles.

5.1. Typical behaviour under loading–unloading paths

The loading–unloading strain–stress curves representing the typical loading–unloading response of the one-dimensional model are presented on the Fig. 5-1. These curves present various typical characteristics:

– three phases in loading describing elasticity, damage alone then damage plus debonding,
– an elastic release,
– a residual strain when loading is completely released,
– a non-symmetrical behaviour between tension and compression, depending on the residual strain.

5.2. Typical behaviour under cyclic loading

The presented model is aimed at representing RC behaviour under cyclic solicitations. In this section we detail the typical response of the model under cyclic solicitations by an alternate symmetrical tensile then compressive then tensile cyclic loading path under strain-control. The strain loading history is drawn in Fig. 5-2.

Fig. 5-3 presents the typical stress–strain response of the model submitted to the strain loading cycles shown on Fig. 5-2.

The stiffness restitution, when the loading evolves from tension to compression, can be observed on Fig. 5-3. This behaviour is related to experimental results where cracks, opened in tension, are progressively closed by the unloading due to the previous steel concrete debonding so that RC seems to be undamaged when the tensile residual strains are equal to zero. Moreover, the observation of hysteretic cycle areas underlines that the major part of dissipation occurs during the first cycle and more precisely during tensile loading step. Indeed, due to the non-symmetrical thresholds in tension and compression, damage process does not occur in
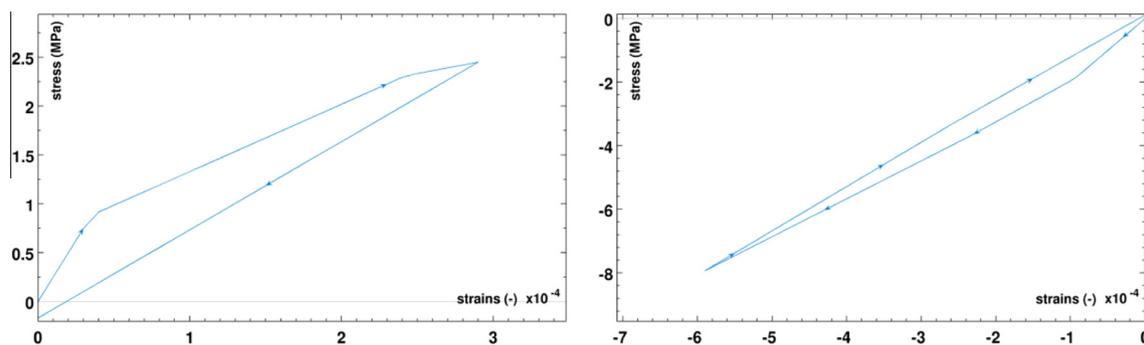

Fig. 5-1. Typical behaviour in tension (left) and compression (right) for damage-debonding model.
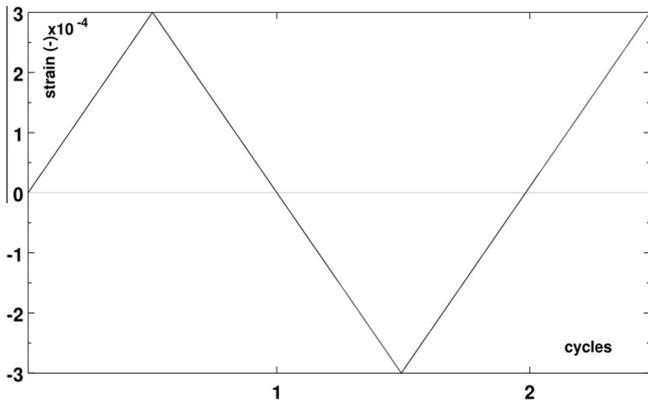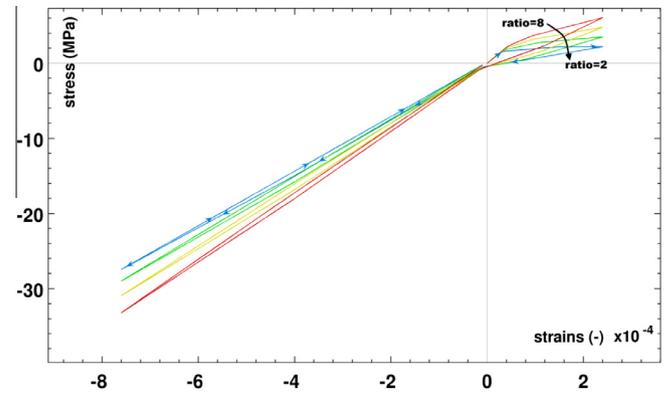
Fig. 5-2. Strain loading history and definition of cycles.

Fig. 5-5. Parametric study on the influence of steel/concrete elastic moduli ratio k^s/k^c.
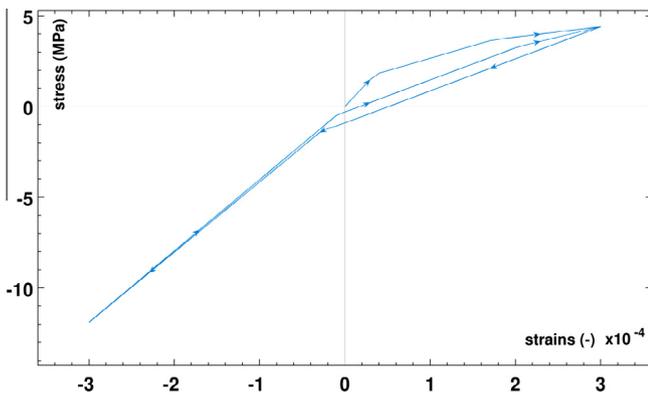

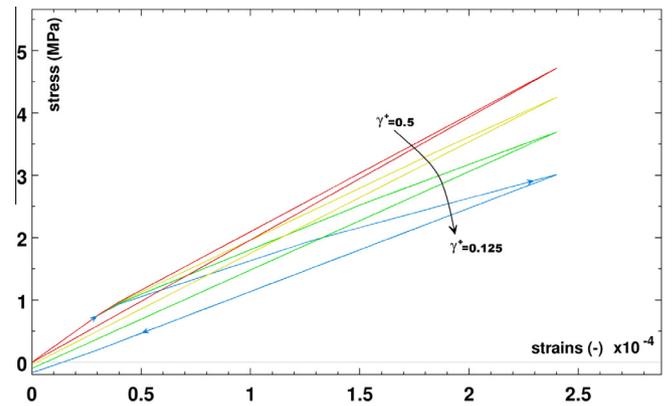Fig. 5-3. Stress–strain curve for a symmetric alternate strain loading with 2 cycles.

Fig. 5-6. Parametric study on the influence of damage parameter γ.
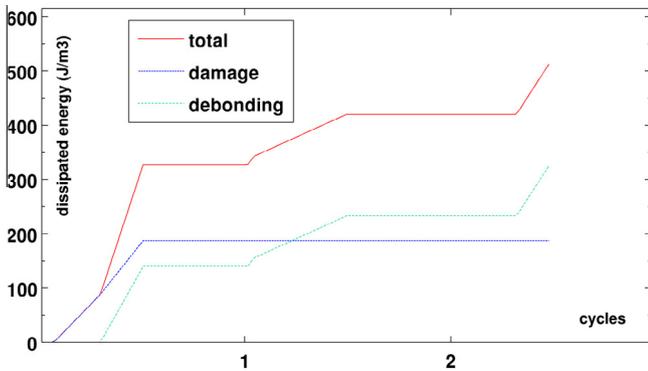

Fig. 5-4. Damage (blue), debonding (green) and total (red) dissipated energy over time for a symmetric alternate loading on two strain-controlled cycles. (For interpretation of the references to colour in this figure caption, the reader is referred to the web version of this article.)

compression because the damage compression threshold is not reached, being much further than the damage tension one.

In order to assess the dissipative properties of this model, the evolution of damage (blue dotted line), debonding (green line) and total (red continuous line) dissipated energies are plotted on Fig. 5-4.

On Fig. 5-4, one can observe that damage only occurs during the first tension cycle while debonding also occurs at the end of each cycle. Thus the introduction of debonding is an efficient way to represent dissipation during the whole cycles. The previous remarks on dissipated energies outline the overall threshold

hardening behaviour of the model which is different for debonding and damage thresholds.

5.3. Parametric study

Once explained the meaning of each parameters and the way to choose it in Section 4, the present section will study their influence on the general shape of typical response curves. In the following, each parameter studied has been modified from 0.5 to 2 times its reference value.

The Table 2 gathers all the reference values used for the parametric study.

The first presented parametric study lies on the ratio k^s/k^c. Indeed, the study of the variation of each stiffness parameter k^c and k^s alone has no real interest for future user and one should focus rather on the study of the ratio steel–concrete stiffness, represented by k^s/k^c. Thanks to these curves, see Fig. 5-5, it is noticeable that this ratio has an influence not only on the post-elastic slope and, consequently on residual strains, but also on the values of both damage and debonding global thresholds. As a consequence, the more steel is present in the studied plate, the more sliding occurs. The proposed model seems so more suitable for representing the behaviour of highly reinforced members.

As for the second study, it focuses on the influence of damage parameter γ. The study has been conducted under tension loading with a reference value of $\gamma_+ = 0.25$. One can see anew the influence of this parameter on the post-elastic slope as well as on the value of debonding threshold, see Fig. 5-6.

Other studies have been conducted on each other parameter listed at the beginning of this section. They only confirm the

Table 2
Model parameters reference values.

k^c(MPa m²)	k^s (MPa m²)	ratio k^s/k^c	$\gamma_+(-)$	$\gamma_-(-)$	σ_{d+}(MPa)	σ_{d-}(MPa)	σ_{crit}(MPa)
40,000	10,000	4	−0.05	0.5	1	2	1

previous remarks: the two parameters σ_{d+} and σ_{d-} influence the tension and compression first damage global thresholds, and σ_{crit} influences the debonding macroscopic threshold.

6. Application of the 1D model: SAFE shear wall experiments

In order to know further about the ability of the presented model of Sections 3 and 4 to properly represent RC panels behaviour subjected to cyclic solicitations and in relation with the final aim of this work (application to RC plates under seismic solicitations), a comparison with experimental results is presented below. This comparison will conclude on the interest of the homogenised plate model presented in Section 2 to be implemented and properly identified.

6.1. Presentation and modeling choices

The chosen application is the SAFE experiments (Brun et al., 2010; Pegon et al., 1998) that were carried out at JRC, Ispra, Italy, on RC walls subjected to pure cyclic shear. Comparisons lean on the results of wall T5 subjected to the first run. This mock up is composed of two stiff RC flanges and a RC web wall 3.00 m long times 1.20 m high, corresponding to a very low aspect ratio equal to 0.4. The web thickness is equal to 20 cm. The wall is constructed with strong blocks up and down, with a large thickness of 1.25 m. Loads are applied by two sets of actuators connected to a steel casing bolted to the upper block. There are 5 hydraulic jacks on the right side and 5 on the left, for a maximum total force of 7 MN. Forces are applied to the steel casing at the mid height of the wall so as to limit rotation of the upper block. In addition, rotation of the upper block is prevented by two vertical actuators at the lateral borders of it. An additional device is introduced in order to generate a normal vertical stress of 0.34 or 1 MPa in shear wall. The lower block is clamped to the laboratory strong floor. The horizontal displacements prescribed at every time-step of the pseudo-dynamic test are measured by optical transducers. Even if the two flanges are loaded by an alternate bending motion, the main structural element, that is the RC web wall, is loaded by an alternate membrane shear.

Considering that the one dimensional presented model of Section 3 is only working in tension–compression and that the SAFE experiments is a shear test, several simplifications are used to idealise the web wall. First of all, based on the work of Kotronis et al. (2003), shear wall is assimilated to two one dimensional RC connecting rods, Poisson's effect being neglected. Through a very simple change in reference frame, the imposed horizontal displacement is so prescribed to these connecting rods at their upper ends A and B whereas their lower ends C and D are clamped. Flanges are not modelised. (see Fig. 6-1).

Parameters are then identified considering Young's moduli for concrete and steel of 28.6 GPa and 200 GPa respectively. Steel proportion of 0.8% and compression and tension concrete failure limits of respectively f_{cm}=46.4 MPa and f_{ct}=3.32 MPa are given by experimental data and from these last values are defined first damage stress limits in compression and tension: σ_{d-} = 10%f_{cm} and σ_{d+} = 40%f_{ct}. Those values are defined arbitrary but related to the following reasonable assessments: concrete in compression starts to damage early but appears to be ductile so the first damage stress limit can be set up at 10% of the compression failure limit, whereas
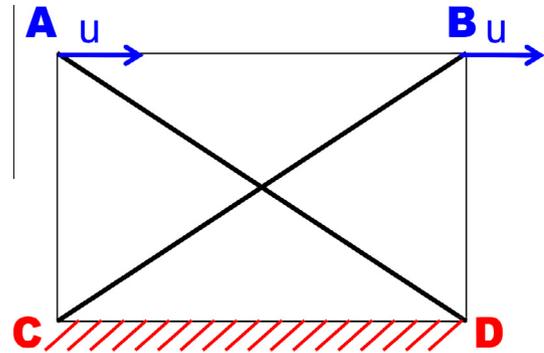

Fig. 6-1. Equivalent RC connecting rods representing SAFE RC wall T5.
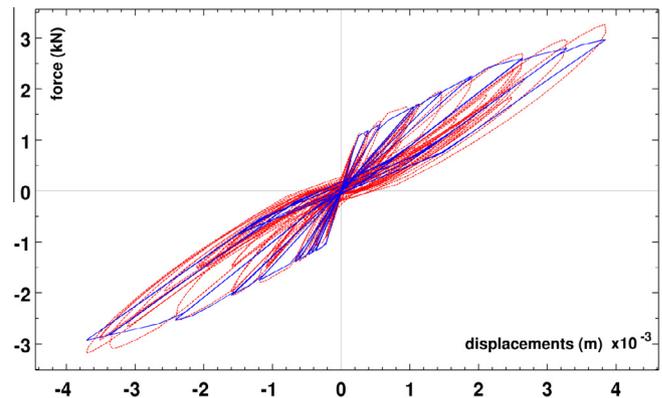

Fig. 6-2. SAFE shear-wall experimental program: wall T5; comparison between test (dotted red line) and model (continuous blue line) results. (For interpretation of the references to colour in this figure caption, the reader is referred to the web version of this article.)

concrete in tension is considered as quasi-fragile and its first damage stress limit should be set up closer to the failure limit in tension. However, the post elastic slope parameter γ_+ for concrete in tension has to respect the condition (4-4) and as a consequence has to be greater than −0.027. The post elastic slope is so very weak and the first damage stress limit is set up at a smaller value than expected. As for first debonding stress for concrete and steel interface, σ_{crit}, it is set up at a value of 1.5 MPa, according to literature and to the consideration that what creates debonding is failure of concrete in tension. Finally, tension and compression damage parameters γ_+ and γ_- are set up thanks to reference curves of concrete in tension and compression to the respective values −0.01 and 0.8.

6.2. Results

Fig. 6-2 presents the macroscopic force–displacement response of the SAFE T5 shear wall with comparison between experimental global force–displacement (dotted red line) and results obtained with simulation using the presented model (continuous blue line). There is a good agreement between experimental response and presented model, especially regarding the envelope, the maximal force and the decrease of global stiffness. However, the residual displacement is underestimated by the model. As a consequence,

in terms of dissipated energy, the presented model is still insufficient, but yet satisfactory. This could be explained by the simplicity of the one dimensional rods modeling and should be corrected by the use of a two-dimensional plate model, based on the analysis proposed in Section 2.

Several other comparisons have been conducted with the damage-only version or a debonding only version of the model. It appears that the combination of these two mechanisms is necessary to properly represent the global behaviour of RC shear wall. Indeed, residual displacements results of debonding whereas the decrease in global stiffness mainly results of damage and the experimental data show these two phenomena. Furthermore, even though the number of parameters could be seen as large (and cannot be reduced), their identification, presented in 4.2, appears to be very accessible to engineers because it lies on measurable variables. As a consequence, the proposed one-dimensional homogenised model of Section 3 seems to present good characteristics to be used easily and efficiently, not only as a validation tool, but also as a prediction one. This validates the interest for implementing the stress resultant RC plate constitutive model obtained by the homogenisation technique presented at Section 2.

7. Conclusion and work in progress

In this paper, we proposed a stress resultant constitutive model representing RC plates global behaviour, coupling damage and debonding, built through averaging periodic homogenisation technique within the framework of the GSM theory. This model is explicitly defined in one dimension (for members) and outlines interesting characteristics as no debonding before damage, a limited number of parameters and a convex free energy. It runs properly on basic numerical tests as well as more sophisticated ones and its typical behaviour shows good agreement to what can be physically observed (stiffness degradation, dissymmetrical behaviour and stiffness restitution between tension and compression, residual strains...). The influence of its parameters on the global shape of the stress–strain response has been studied. Finally, a comparison with an experimental wall subjected to quasi-pure shear, through the example of the SAFE experiments, is satisfactory; however, a small lack of energy dissipation is observed. Indeed, this one dimensional version of the constitutive model is a first approach of periodic homogenisation for RC one dimensional member, so the comparison with a RC panel cannot be so realistic.

On the basis of this study, the implementation of the constitutive model dedicated to plates presented in Section 2 is in progress. As a closed-form resolution of the five cellular three-dimensional problems (2-6) appears to be impossible, FEM numerical simulations will be run on the periodic unit cell and homogenised factors, with their dependence on D, will be identified from them by a basic least square identification. The three-dimensional periodic unit cell will be defined from the material and geometric characteristics of the studied RC plate. Regarding the primary results of the one-dimensional model, the so-created plate model is expected to present satisfying behaviour as well as quite limited number of parameters necessary to determine macroscopic behaviour of RC panels in membrane plus bending coupling damage and debonding under cyclic loading.

Acknowledgement

References

Alliche, A., Dumontet, H., 2011. Anisotropic model of damage for geomaterials and concrete. Int. J. Numer. Anal. Methods Geomech. 35 (9), 969–979.

Amadio, C., Fragiacomo, M., 1993. A finite element model for the study of creep and shrinkage effects in composite beams with deformable shear connections. Costruzioni Metalliche 4, 213–228.

Andrieux, S., Bamberger, Y., Marigo, J.J., 1986. Un modèle de matériau microfissuré pour les roches et les bétons. J. Méca. Théo. Appl. 5, 471–513.

Badel, P., Godard, V., Leblond, J.-B., 2007. Application of some anisotropic damage model to the prediction of the failure of some complex industrial concrete structure. Int. J. Solids Struct. 44, 5848–5874.

Banon, H., Irvine, H.M., Biggs, J.M., 1981. Seismic damage in reinforced concrete frames. J. Struct. Div. 107 (9), 1713–1729.

Brun, M., Labbé, P., Bertrand, D., Courtois, A., 2010. Pseudo-dynamic tests on low-rise shear walls and simplify models based on structural frequency drift. Eng. Struct. 33, 796–812.

Brun, M., Reynouard, J.M., Jezequel, L., 2003. A simple shear wall model taking into account stiffness degradation. Eng. Struct. 25, 1–9.

Caillerie, D., 1984. Thin elastic periodic plates. Math. Methods Appl. Sci. 6, 159–191.

Caillerie, D., 1995. 2D models of plate-like 3D elastic bodies. In: Asymptotic Theories for Plates and Shells. Pitman Res. Notes in Math. S., vol. 319. Longman Sc. & Tech., pp. 28–34.

Carpinteri, A., Carpinteri, A., 1984. Hysteretic behaviour of RC beams. ASCE J. Struct. Eng. 110 (9), 2073–2084.

CEB-FIP, 1993. Model Code for concrete structures. CEB Bulletin d'Information, Comité Euro International du Béton, Lausanne, Switzerland.

Chaboche, J.L., 2003. Damage mechanics. In: Milne, I., Ritchie, R.O., Karihaloo, B. (Eds.), Comprehensive Structural Integrity, vol. 2. Elsevier Ltd, Oxford, pp. 213–284.

Coleman, B.D., Gurtin, M., 1967. Thermodynamics with internal variables. J. Chem. Phys. 48 (2), 597–613.

Dragon, A., Mroz, Z., 1979. A continuum model for plastic-brittle behaviour of rock and concrete. Int. J. Eng. Sci. 17, 121–137.

Fardis, M.N., 2009. Seismic Design, Assessment and Retrofitting of Concrete Buildings. Springer Verlag, Dordrecht.

Farrar, C.R., Baker, W.E., 1992. Measuring the stiffness of concrete shear walls during dynamic tests. Exp. Mech., 179–183, June.

Favre, R., Jaccoud, J.P., Burdet, O., Charif, H., 1990. Traité de génie civil de l'École Polytechnique fédérale de Lausanne.

Feenstra, P.H., De Borst, R., 1995. Constitutive model for reinforced concrete. J. Eng. Mech. 121 (5), 587–595.

Gatuingt, F., Pijaudier-Cabot, G., 2002. Coupled damage and plasticity modeling in transient dynamic analysis of concrete. Int. J. Numer. Anal. Methods Geomech. 26, 1–24.

Germain, P., 1973a. Mécanique des Milieux Continus. Masson, Paris.

Germain, P., 1973b. The method of virtual power in continuum mechanics, part 2: microstructure. SIAM J. Appl. Math. 25 (3), 556–575.

Germain, P., Nguyen, Q.S., Suquet, P., 1983. Continuum thermodynamics. ASME J. Appl. Mech. 50, 1010–1021.

Goto, Y., 1971. Cracks formed in concrete around deformed tension bars. J. ACI 68 (4), 224–251.

Guedes, J., Pegon, P., Pinto, A., 1994. A fibre Timoshenko beam element in Castem2000. Special publication Nr. I.94.31, Joint Research Center, I-21020 Ispra, Italy.

Halphen, B., Nguyen, Q.S., 1975. Sur les matériaux standards généralisés. J. de Mécanique 14, 39–63.

Hill, R., 1972. On constitutive macro-variables for heterogeneous solids at finite strain. Proc. R. Soc. London, Ser. A 326, 131–147.

Ingraffea, A.R., Gerstk, W.H., Gergely, P., Saouma, V., 1984. Fracture mechanics of bond in reinforced concrete. ASCE J. Struct. Eng. 110 (4), 871–890.

Kobayashi, A.S., Hawkins, N.M., Chan, Y-L.A., Lin, I.J., 1980. A feasibility study of detecting reinforcing-bar debonding by acoustic-emission technique. Exp. Mech. September, 301–308.

Koechlin, P., Potapov, S., 2007. Global constitutive model for reinforced concrete plates. ASCE J. Eng. Mech. 133 (3), 257–266.

Kotronis, P., Mazars, J., Davenne, L., 2003. The equivalent reinforced concrete model for simulating the behavior of walls under dynamic shear loading. Eng. Frac. Mech. 70 (7–8), 1085–1097.

Krätzig, W., Polling, R., 2004. An elasto–plastic damage model for reinforced concrete with minimum number of material parameters. Comput. Struct. 82, 1201–1215.

Lee, H.P., 2011. Shell finite element of reinforced concrete for internal pressure analysis of nuclear containment building. Nucl. Eng. Des. 241, 515–525.

Lemaître, J., Chaboche, J.-L., 1990. Mechanics of Solid Materials. Cambridge University Press.

Lorentz, E., Andrieux, S., 2003. Analysis of nonlocal models through energetic formulations. Int. J. Solids Struct. 42 (12), 2905–2936.

Lorentz, E., Godard, V., 2011. Gradient damage models: toward full-scale computations. Comput. Methods Appl. Mech. Eng. 200 (21–22), 1:1927–1:1944.

Maekawa, K., Pimanmas, A., Okamura, H., 2003. Nonlinear Mechanics of Reinforced Concrete. Spon Press, London.

Markovic, D., Koechlin, P., Voldoire, F., 2007. Reinforced concrete structures under extreme loading: Stress resultant Global Reinforced Concrete Models (GLRC). In: COMPDYN 2007 – Comput. Meth. in Struct. Dyn. and Earthq. Eng., Paper 1319.

Marti, P., Alvarez, M., Kaufmann, W., Sigrist, V., 1998. Tension chord model for structural concrete. Struct. Eng. Int. 98 (4), 287–298.

Mazars, J., Kotronis, P., Davenne, L., 2002. A new modeling strategy for the behaviour of shear walls under dynamic loading. Earthquake Eng. Struct. Dyn. 31, 937–954.

Mörsch, E., 1909. Concrete-Steel Construction. McGraw-Hill, New York.

Nedjar, B., 2001. Elastoplastic-damage modeling including the gradient of damage. Formulation and computational aspects. Int. J. Solids Struct. 38, 5421–5451.

Ngo, D., Scoderlis, A.C., 1967. Finite element analysis of reinforced concrete beams. ACI J. 64, 152–163.

Okamura, H., Kim, I.H., 2000. Seismic performance check and size effect FEM analysis of reinforced concrete. Eng. Fract. Mech. 65, 369–389.

Pascu, I.R., 1995. Contribution à l'analyse d'éléments en béton armé sollicités en membrane et flexion bi-axiale. Thèse, INSA Lyon, France.

Pegon, P., Magonette, G., Molina, F.J., Verzeletti, G., Dyngeland, T., Negro, P., Tirelli, D., Tognoli, P., 1998. Programme SAFE: Rapport du test T5. EC, Joint Research Center, I-21020 Ispra, Italy.

Perić, D., de Souza Neto, E.A., Feijóo, R.A., Partovi, M., Carneiro Molina, A.J., 2011. On micro-to-macro transitions for multi-scale analysis of non-linear heterogeneous materials: unified variational basis and finite element implementation. Int. J. Numer. Methods Eng. 87 (1–5), 149–170.

Pijaudier-Cabot, G., Bažant, Z., 1987. Nonlocal damage theory. J. Eng. Mech. 113 (10), 1512–1533.

Pimentel, M., Brühwiler, E., Figueiras, J., 2010. Extended cracked membrane model for the analysis of RC panels. Eng. Struct. 32, 1964–1975.

Reinhardt, H., Cornelissen, H., Hordijk, D., 1986. Tensile tests and failure analysis of concrete. J. Struct. Eng. 112 (11), 2462–2477.

Rumanus, E., Meschke, G., 2007. Homogenization-based modeling of reinforced concrete in the context of durability-oriented analyses. In: ECCOMAS Thematic Conference on Computational Methods in Structural Dynamics and Earthquake Engineering, Rethymno, Crete, Greece.

Rumanus, E., Meschke, G., 2008. Modeling of reinforced concrete by means of homogenization approach including steel–concrete interactions. In: WCCM8, Venice.

Rutenberg, A., 1982. Simplified P-Delta analysis for asymmetric structures. ASCE J. Struct. Div. 108-9, 1995–2013.

Sanchez-Palencia, E., 1980. Non-Homogeneous Media and Vibration Theory, Vol. 127. Springer, Heidelberg.

Sanchez-Palencia, E., Zaoui, A., Suquet, P., 1987. Homogenization Technique for Composite Media. Springer, Berlin Heidelberg.

Sheikh, S.A., Uzumeri, S.M., 1982. Analytical model for concrete confinement in tied columns. ASCE J. Struct. Div. 108 (12), 2703–2722.

Selby, R.G., Vecchio, F.J., 1997. A constitutive model for analysis of reinforced concrete solids. Can. J. Civ. Eng. 24, 460–470.

Shao, J.F., Jia, Y., Kondo, D., Chiarelli, A.S., 2006. A coupled elastoplastic damage model for semi-brittle materials and extension to unsaturated conditions. Mech. Mater. 38, 218–232.

Soltani, M., An, X., Maekawa, K., 2003. Computational model for post cracking analysis of RC membrane elements based on local stress–strain characteristics. Eng. Struct. 25, 993–1007.

Soltani, M., An, X., Maekawa, K., 2005. Localized nonlinearity and size-dependent mechanics of in-plane RC element in shear. Eng. Struct. 27, 891–908.

Spacone, E., Filippou, F.C., Taucer, F.F., 1996. Fiber beam column model for nonlinear analysis of RC frames. I: Formulation.. Earthquake Eng. Struct. Dyn. 25 (7), 711–725.

Spacone, E., El-Tawil, S., 2004. Nonlinear analysis of steel–concrete composite structures: state of the art. J. Struct. Eng. 130, 159–168.

Stolz, C., 2010. On micro-macro transition in non-linear mechanics. Materials 3, 296–317.

Suquet, P., 1982. Plasticité et homogénéisation. Thèse d'Etat, Université Paris VI.

Suquet, P., 1993. Overall potentials and extremal surfaces of power law or ideally plastic composites. J. Mech. Phys. Solids 41, 981–1002.

Vecchio, F.J., Collins, M.P., 1986. Modified compression field theory for reinforced concrete elements subjected to shear. ACI J. 83, 219–231.

Takeda, T., Sozen, M.A., Nielsen, N., 1970. Reinforced concrete response to simulated earthquakes. J. Struct. Div. 96 (12), 2557–2573.